

See discussions, stats, and author profiles for this publication at: <https://www.researchgate.net/publication/231376429>

Critical-Point Temperature of Ionic Liquids from Surface Tension at Liquid–Vapor Equilibrium and the Correlation with the Interaction Energy

ARTICLE in INDUSTRIAL & ENGINEERING CHEMISTRY RESEARCH · OCTOBER 2010

Impact Factor: 2.59 · DOI: 10.1021/ie1013772

CITATIONS

14

READS

100

4 AUTHORS, INCLUDING:



Mohammad Hadi Ghatte

Shiraz University

71 PUBLICATIONS 741 CITATIONS

SEE PROFILE



Fatemeh Moosavi

Ferdowsi University Of Mashhad

25 PUBLICATIONS 243 CITATIONS

SEE PROFILE



Amin Reza Zolghadr

Shiraz University

18 PUBLICATIONS 248 CITATIONS

SEE PROFILE

Critical-Point Temperature of Ionic Liquids from Surface Tension at Liquid–Vapor Equilibrium and the Correlation with the Interaction Energy

Mohammad Hadi Ghatee,* Fatemeh Moosavi, Amin Reza Zolghadr, and Razyeh Jahromi

Department of Chemistry, Shiraz University, Shiraz 71454, Iran

The critical temperature of ionic liquids is predicted by scaling-law, Guggenheim, and Eötvös approaches, using surface tension data measured in the temperature range of 293–393 K. The available surface tension data for imidazolium-, phosphonium-, and ammonium-based ionic liquids, with different anions content, show that the predicted critical temperature is a function of cation type and its alkyl chain length as well as the anion type. According to this dependence on the nature of the ionic liquid, the anion–cation interaction energy (E_{inter}) was calculated by quantum mechanical density functional theory and the correlation with the predicted critical temperature was studied. The predicted critical temperature has a direct correlation to the absolute value of E_{inter} . The ionic liquids with the BF_4^- anion, which consistently have the highest critical point temperature, also have the largest absolute value of E_{inter} . As the alkyl chain length increases, the critical temperature decreases. When the surface tension is measured under a liquid–vapor equilibrium, the prediction has the meaningful feature of producing the critical-point temperature.

1. Introduction

In the development of less-polluting solvents, their liquidus range is the key element in the promising endeavor for sustainable industrial progress.^{1,2} Since the time it was professed that the designer solvents/ionic liquids might boost clean technology development, these liquids have received most of the attention, because of their thermophysical properties.³

Ionic liquids (ILs), which are organic salts with a low melting point, have advantages that include very low volatility, wide tunable properties (with regard to polarity, hydrophobicity, and nontoxicity), and a wide liquidus temperature range.⁴ Many growing rapidly applications of ILs include organic product extraction,⁵ use as reaction media for organic synthesis,⁶ electrochemical reactivity,⁷ extraction processes,⁸ and catalysis and biocatalysis.^{9,10}

The large number of available cations and anions allow a wide range of physical and chemical characteristics to be achieved. Most ILs are based on 1,3-dialkylimidazolium or *N*-alkylpyridinium cations and halogenated counteranions, such as hexafluorophosphate (PF_6^-), tetrafluoroborate (BF_4^-), bis(trifluoromethanesulfonyl) imide $[(\text{CF}_3\text{SO}_2)_2\text{N}^-]$, and their derivatives. Halogens are appreciably effective in reducing negative charge density, because of their electron-withdrawing effect.

Applications of these ILs demand tremendous amounts of work for the knowledge of their thermophysical properties. Although many physical properties of ILs (including melting temperature, density, surface tension, gas solubility, viscosity, conductivity, refractive index, and their temperature dependence) have been studied recently,^{11–13} there is scarce information about their critical properties. The behavior of a fluid near its critical point is a specific property necessary to develop the thermodynamic models for fluids. Critical parameters are often used for industrial reactor design. The factors that influence the values of these parameters for ILs must be viewed by the effect of short-range van der Waals interactions as well as the electrostatic interactions. The critical properties cannot be determined experimentally, because many of these compounds decompose

as the temperature approaches the normal boiling point; due to such limitation, strategies to determine the critical properties of ILs have not received much attention in the literature.¹⁴ Thus, much work still remains to be done to extend the existing IL database and gain better insight into the physicochemical properties of such compounds.

The existing empirical scaling laws elucidate the surface tension close to the critical temperature as a function of the temperature-scaled distance from the critical temperature. The scaling law comprises a definite power law with characteristic exponents.^{15,16}

Recently, models applicable to normal fluids have been used to study and estimate the critical temperature of the ILs. Rebelo et al.¹⁷ have predicted the critical temperatures of several ILs, based on experimental surface tension and density data, using the Eötvös and Guggenheim empirical equations. The adequacy of the method has been ensured by testing a set of 90 compounds with known critical temperature (T_c) and/or boiling temperature (T_b) values, ranging from quantum liquids, to molten inorganic salts, to inorganic and organic compounds with strong hydrogen bonding. They have also provided estimations of the normal T_b and T_c values for 15 ionic liquids, with an accuracy that has been claimed to be better than 10%. Exceptions to this accuracy in the prediction of the T_c and T_b values are observed for water, light alcohols, and a few inorganic molten salts.

Valderrama et al.¹⁴ have predicted the critical properties, the normal boiling temperatures, and the acentric factors of 250 ILs, using an extended group contribution method. Because of the unavailability of experimental critical properties, they have checked the accuracy of the method using the calculated liquid densities. The critical characteristics obtained were applied to estimate the liquid bulk density. They have also mentioned that the ratio of T_b/T_c is not quite in agreement with the results of Rebelo et al.,¹⁷ who have used that as a criterion for the validity of the critical point.

More recently, Weiss and co-workers¹⁸ have predicted the critical temperature for 1-butyl-3-methylimidazolium hexafluorophosphate ($[\text{C}_4\text{mim}]\text{PF}_6$) from the surface tension data. They evaluated four datasets; nevertheless, they favored the surface tension data of the present authors,^{19a} which, unlike the other

* To whom correspondence should be addressed. Tel.: +98 711 613 7353, +98 711 228 4822. Fax: +98 711 228 6008. E-mail: ghatee@susc.ac.ir.

sets, have been measured under liquid–vapor equilibration. The estimate of the critical temperature— $T_c = 1100 \pm 100$ K for $[C_n\text{mim}]\text{PF}_6$, which approaches and agrees well with the results of Rebelo et al.¹⁷ at $T_c = 1100$ – 1180 K and with the result of their YASP molecular dynamics (MD) simulation—involves data points at much higher temperatures than the available experimental data. Therefore, if the experimental data up to 400 K or the simulated data up to 800 K are extrapolated by the Guggenheim relation, the predicted critical point would remain almost unchanged.

Carvalho et al.²⁰ have reported surface tension data for six imidazolium-, pyridinium-, pyrrolidinium-, and phosphonium-based ILs that contain the TF_2N^- anion in the temperature range of 293–353 K at atmospheric pressure. They have predicted T_c values using both the Eötvös and Guggenheim equations.

On the other hand, in some studies, the experimental values of several physical properties have been compared with the molecular structural properties using *ab initio* calculations. Turner and co-workers²¹ have studied and suggested a relationship between the structure and the melting point of ILs. They have also calculated the interaction energies for 1-alkyl-3-methylimidazolium halides via *ab initio* methods, and they have demonstrated a closely corresponding relationship with the known X-ray crystal structure.

As a part of systematic studies on liquid surface properties,^{19a,22} first, we use the temperature dependence data of the experimental surface tension over a wide range of temperatures to estimate the T_c values of different ILs that are based on imidazolium, phosphonium, and ammonium cations. We then study the correlation between the T_c value, which can be predicted directly from the experimental data, and a structural property (e.g., interaction energy, which is deduced from quantum mechanical density functional theory (DFT)). The use of surface tension values measured under liquid–vapor equilibration has a significant feature of producing a critical-point temperature. Rebelo et al.¹⁷ have mentioned that the accuracy of vapor pressure when it is designed to examine the macroscopic behavior via studies at a molecular level is important. The vapor pressure (and its dependence on the temperature) of a condensed phase are among those fundamental properties needed to contribute to the development and testing of accurate molecular models. On the other hand, the liquid–vapor critical parameters are required for the implementation of the corresponding equation of state (EoS) correlations.

2. Evaluation of Critical Temperature

The inherent possibility of accurate measurement of the liquid surface tension (γ) turns into a strong and reliable method of studying the liquid surface energetics and surface microstructure.²³ The liquid surface tension linearly decreases at low temperatures close to the freezing point and vanishes nonlinearly as the critical point is approached. Consequently, under circumstances in which the experimental determination of the T_c values of thermally unstable compounds is not possible, an alternative is its reliable estimation from the surface tension data directly.

In the modern theory of critical phenomena, the liquid surface tension can be given by the scaling law, as

$$\gamma = \gamma_0 \tau^\mu \quad (1)$$

where γ_0 is a substance-dependent constant, μ the critical exponent of the surface tension, and τ the reduced temperature ($\tau = 1 - (T/T_c)$, where T_c is the critical temperature). For all

normal fluids and their mixtures,^{22,24} the scaling law is valid, with a characteristic exponent of $\mu = 1.26$. The properties of the scaling law and the critical exponent can be supported by experimental data.

According to Guggenheim,²⁵ a certain exponent describes the vanishing of surface tension with the temperature and is universally applied to compounds of the same universality class, irrespective of their chemical nature. Similar to the scaling law, the temperature-dependent surface tension can be described by

$$\gamma = a(T_c - T)^{11/9} \quad (2)$$

where a is a substance-dependent constant. However, note that a simple and accurate power law such as the Guggenheim relation is not guaranteed to be valid over all temperatures range down to the triple point.

One of the earliest and best-known empirical relations that involve the temperature dependence of surface tension is that of Eötvös:

$$\gamma \left(\frac{M}{\rho} \right)^{2/3} = k(T_c - T) \quad (3)$$

where k is a constant, ρ the liquid density (given in units of g/cm^3), and M the molecular mass (expressed in units of g/mol).

In this work, surface tension data were used to estimate the critical temperature of some ILs, using eqs 2 and 3.

3. Computational Details

The usual procedure of quantum mechanical DFT was performed to determine the interaction energy between the cation and the anion. The initial structure of each IL was prepared and the geometry optimized by classical molecular mechanics simulation. Subsequently, using the Gaussian 03 package,²⁶ further optimization for the final stable molecular structure was carried out by quantum mechanical DFT at the B3LYP/6-311G** level of theory. The final structure was fully characterized as minima by frequency analysis. This allows verification of the adequacy of the B3LYP method and the 6-311G** basis set to attain stable minima. The results of calculations using the B3LYP functional were determined to be reliable when compared with the literature structural information.^{21,27} Our experience has shown that basis set superposition error (BSSE) influences the results inappreciably.

Next, a systematic approach was used to calculate the anion–cation interaction energy (E_{inter}), which is defined as the difference between the energy of the pair of ionic system (E_{AX}) and the sum of the energies of the purely cationic (E_{A^+}) and anionic (E_{X^-}) species:

$$E_{\text{inter}} (\text{kJ/mol}) = 2625.50[E_{\text{AX}}(\text{au}) - E_{\text{A}^+}(\text{au}) - E_{\text{X}^-}(\text{au})] \quad (4)$$

For this purpose, each isolated IL and its corresponding cation and anion were optimized for structure and energy at the B3LYP/6-311G** level of theory, as mentioned above.

The calculations were performed on 12 ILs: $[C_n\text{mim}]\text{BF}_4$, $[C_n\text{mim}]\text{PF}_6$, $[C_n\text{mim}]\text{I}$, and $[C_n\text{mim}]\text{Cl}$, where $n = 4, 6$, and 8. These calculations include 10 ILs for which the interfacial tension at the liquid–vapor equilibrium has been measured experimentally in our previous work.^{19a}

4. Results and Discussion

4.1. Estimation of Critical Temperature. We used three approaches (eqs 1–3) to calculate the critical temperature (T_c)

Table 1. Density Values for the Imidazolium-Based Ionic Liquids (ILs) under Study¹⁹

temperature, <i>T</i> (K)	Density (g/cm ³)									
	[C ₄ mim]I	[C ₄ mim]Cl	[C ₄ mim]PF ₆	[C ₄ mim]BF ₄	[C ₆ mim]I	[C ₆ mim]Cl	[C ₆ mim]PF ₆	[C ₆ mim]BF ₄	[C ₈ mim]Cl	[C ₈ mim]BF ₄
298.15	1.450	1.092	1.378	1.154	1.328	1.049	1.311	1.100	1.019	1.038
303.15	1.448	1.091	1.375	1.152	1.326	1.047	1.308	1.097	1.017	1.032
308.15	1.446	1.089	1.373	1.148	1.324	1.045	1.305	1.094	1.015	1.028
313.15	1.444	1.086	1.369	1.144	1.322	1.043	1.301	1.090	1.013	1.024
318.15	1.442	1.084	1.364	1.140	1.320	1.041	1.298	1.087	1.009	1.020
323.15	1.440	1.082	1.360	1.136	1.318	1.038	1.294	1.084	1.006	1.016
328.15	1.438	1.080	1.357	1.134	1.316	1.036	1.289	1.082	1.004	1.012
333.15	1.436	1.076	1.351	1.130	1.314	1.035	1.287	1.080	1.002	1.008
338.15	1.434	1.073	1.348	1.128	1.312	1.031	1.284	1.078	0.997	1.004
343.15	1.432	1.072	1.344	1.124	1.310	1.028	1.280	1.074	0.995	1.000
348.15	1.430	1.070	1.340	1.120	1.308	1.023	1.275	1.070	0.992	0.996
353.15	1.428	1.068	1.336	1.116	1.306	1.021	1.272	1.068	0.990	0.992
358.15	1.426	1.066	1.332	1.114	1.304	1.020	1.268	1.064	0.988	0.988
363.15	1.424	1.063	1.328	1.110	1.302	1.015	1.264	1.060	0.985	0.984
368.15	1.422	1.062	1.324	1.106	1.300	1.014		1.058	0.982	0.980
373.15	1.420	1.061	1.320	1.102	1.298	1.011		1.056	0.979	0.976
378.15	1.418	1.061	1.316	1.100	1.296	1.008		1.052	0.976	0.972
383.15	1.416	1.059	1.310	1.098	1.294	1.005		1.048	0.973	0.968
388.15	1.414	1.057	1.308	1.094	1.292	1.003		1.044	0.968	0.964
393.15	1.412	1.055	1.306	1.090	1.290	1.001		1.040	0.962	0.960

Table 2. Predicted Critical Point Temperatures and Parameters of Eqs 2 and 3 for Imidazolium-Based ILs^{19a,28}

IL	Guggenheim Parameters			Eötvös Parameters		
	<i>a</i>	critical temperature, <i>T_c</i> (K)	<i>R</i> ²	<i>k</i>	critical temperature, <i>T_c</i> (K)	<i>R</i> ²
[C ₄ mim]I	0.0154	1082.5	0.9986	2.3629	1025.4	0.9982
[C ₆ mim]I	0.0141	1012.3	0.9996	2.4023	959.6	0.9994
[C ₄ mim]Cl	0.0123	1172.2	0.9983	1.6477	1159.6	0.9947
[C ₆ mim]Cl	0.0107	1163.2	0.9992	1.5188	1214.4	0.9985
[C ₈ mim]Cl	0.0106	1000.8	0.9990	1.6413	1020.1	0.9990
[C ₄ mim]PF ₆	0.0136	1092.4	0.9990	1.9424	1151.2	0.9987
[C ₆ mim]PF ₆	0.0134	1043.9	0.9989	2.1322	1078.4	0.9980
[C ₈ mim]PF ₆	0.0123	988.4	0.9960			
[C ₄ mim]BF ₄	0.0102	1230.2	0.9987	1.3739	1366.9	0.9984
[C ₆ mim]BF ₄	0.00924	1227.0	0.9990	1.4179	1339.2	0.9988
[C ₈ mim]BF ₄	0.00928	1055.0	0.9994	1.4441	1189.7	0.9990

from the temperature-dependent surface tension data. However, since the scaling law and the Guggenheim approach are very similar quantitatively, only the results for the Guggenheim and Eötvös approaches will be presented.

The experimental surface tension data were taken from our previous work^{19a} on 10 imidazolium-based ILs, consisting of [C₄mim]⁺, [C₆mim]⁺, and [C₈mim]⁺ cations and I[−], Cl[−], PF₆[−], and BF₄[−] anions in the temperature range of 298–393 K. These data have been measured under liquid–vapor equilibration via the capillary rise method. For [C₈mim]PF₆, the surface tension data of Pereiro et al.,²⁸ based on predictions using the Parachor method in the temperature range of 288–313 K, were used.

The corresponding densities of synthesized ILs, by our group,¹⁹ are listed in Table 1. The details regarding measurement of the density have been given in ref 19b. Using the Guggenheim and Eötvös approaches, the *T_c* values of 11 ILs were predicted and are shown in Table 2.

The *T_c* values that are determined by the two methods are similar. The differences can be attributed to the differences in the accuracy of the methods and the accuracy in the liquid density measurement that must be applied in the Eötvös method. Despite this observation, good agreement between these two methods can be regarded as proof of the credibility of the approaches. As it can be seen from Table 2, the *T_c* values show a systematic variation with cation size, in terms of alkyl chain length, and with the anion type. For instance, the *T_c* values for ILs that contain BF₄[−] anions are the highest and *T_c* decreases as

the alkyl chain length increases. For a given alkyl chain length, the *T_c* values among the anions are ranked in the following order:

$$\text{BF}_4^- > \text{Cl}^- > \text{PF}_6^- > \text{I}^-$$

The trend in terms of alkyl chain length is consistent with Rebelo's et al. results,¹⁷ although the present results of the predicted critical temperatures are higher. The differences can be attributed to the narrow range of temperature (just 30 K) used by Rebelo et al.¹⁷

For a more-reliable estimate of the hypothetical critical-point temperature, Weiss and co-workers¹⁸ have simulated the liquid/vapor interface of [C₄mim]PF₆ up to 800 K, which is a temperature well beyond the thermal stability limit of the real substance. Then, using the Guggenheim and Eötvös approaches, they found very good agreement between the predicted *T_c* values using the surface tension measured at liquid–vapor equilibrium^{19a} and their simulated results. The measured surface tension at liquid–vapor equilibrium was determined to be preferentially favorable. Therefore, it can be expected that the prediction of the critical temperature of ILs using the surface tension data measured at liquid–vapor equilibrium (shown in Table 1 of ref 19a) can be meaningfully regarded as the critical-point temperature (see Table 2).

In developing the approach, a wide variety of ILs, including phosphonium and ammonium with different types of anions (such as InCl₄[−], Tf₂N[−], TFSO₃[−], MeSO₄[−], EtSO₄[−], OcSO₄[−], and PF₃(CF₂CF₃)[−]), in addition to the halides and fluorinated anions, were employed. The selected surface tension data of the ILs^{28–38} are the most reliable datasets over a relatively wide range of temperatures measured by different methods on the liquid at equilibrium with air under ambient pressure or under inert gas atmosphere. (See Table 3 for details.) The calculated *T_c* values and the corresponding parameters, in addition to the uncertainty of the estimate, are given in Table 3. Also, the correlation coefficients (*R*²) of the fits are listed, which are well above the acceptable limit (0.995), except for that observed for [C₁mim]MeSO₄ and [C₄mim]OcSO₄. This can be attributed to the small number of data points available for fitting. For ILs with a Tf₂N[−] anion content, the *T_c* values decrease as the alkyl chain length increases. The decrease in the trend of *T_c* is rather smooth, except that for [C₆mim]Tf₂N, which shows some deviations. Our *T_c* estimates are higher than those reported by Rebelo et al.¹⁷ It might be worthwhile to mention that Weiss³⁹

Table 3. Parameters of Guggenheim Approach (eq 2) Used for Other ILs with Various Anions and Cations

ionic liquid	<i>a</i>	<i>T_c</i> (K)	uncertainty of estimate	<i>R</i> ²	ref	technique ^a	temperature range (K)
[C ₂ mim]Tf ₂ N	0.00894	1300.3	0.0286	0.9978	31	ring method at IL in air	298–350
[C ₃ mim]Tf ₂ N	0.00964	1107.6	0.0772	0.9962	33	ring method at atmospheric pressure	293–353
[C ₄ mim]Tf ₂ N	0.00936	1093.2	0.0495	0.9987	34	pendant drop under air	278–333
[C ₅ mim]Tf ₂ N	0.00995	1051.1	0.0449	0.9988	33	ring method at atmospheric pressure	293–353
[C ₆ mim]Tf ₂ N	0.00933	1156.1	0.0247	0.9992	31	ring method at IL in air	298–350
[C ₇ mim]Tf ₂ N	0.01206	925.2	0.0670	0.9983	33	ring method at atmospheric pressure	293–353
[C ₈ mim]Tf ₂ N	0.01221	917.7	0.0702	0.9978	33	ring method at atmospheric pressure	293–353
[C ₁₀ mim]Tf ₂ N	0.01337	875.8	0.0844	0.9973	33	ring method at atmospheric pressure	293–353
[N ₄ 111]Tf ₂ N	0.00618	1559.3	0.0315	0.9973	31	ring method under dry nitrogen	298–350
[N ₆ 111]Tf ₂ N	0.01232	982.2	0.0440	0.9972	31	ring method under dry nitrogen	298–350
[N ₄ 113]Tf ₂ N	0.01065	1111.8	0.0227	0.9983	31	ring method under dry nitrogen	298–350
[N ₆ 222]Tf ₂ N	0.01530	860.7	0.1108	0.9939	31	ring method under dry nitrogen	298–350
[P ₁₄ 666]Tf ₂ N	0.01627	805.9	0.0718	0.9977	31	ring method at IL in air	298–350
[P ₁₄ 666]Cl	0.01652	806.0	0.0597	0.9982	31	ring method at IL in air	298–350
[C ₁ mim]MeSO ₄	0.01427	1219.8	0.1572	0.9739	35	hanging drop	288–313
[C ₄ mim]MeSO ₄	0.02947	690.5	0.2542	0.9980	36	hanging drop	283–313
[C ₂ mim]TfSO ₃	0.00575	1815.7	0.0362	0.9976	31	ring method at IL in air	298–350
[C ₂ mim]EtSO ₄	0.01547	1005.2	0.0674	0.9953	37	hanging drop	288–313
[C ₄ mim]OcSO ₄	0.01197	849.2	0.1290	0.9918	34	pendant drop under air	278–333
[C ₆ mim]InCl ₄	0.01042	1172.5	0.1102	0.9908	32	forced bubble under dry argon	283–338
[C ₂ OHmim]BF ₄	0.01112	1779.7	0.2505	0.9965	30	pendant drop under air	298–470
[C ₃ mim]PF ₆	0.01279	1139.1	0.1051	0.9908	29	ring method for IL in air at atmospheric pressure	287–353
[C ₂ mim]PF ₃ (CF ₂ CF ₃) ₃	0.00687	1368.4	0.0422	0.9960	38	forced bubble under dry argon	283–338

^a Techniques used for surface tension measurements.**Table 4. Comparison between the Predicted Critical Temperatures by Current Study, Data from Rebelo et al.,¹⁷ and Data from Weiss³⁹**

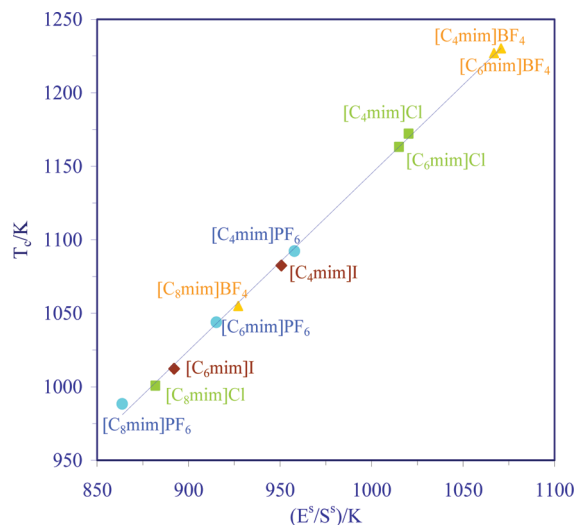
ionic liquid	Critical Temperature, <i>T_c</i> (K)					
	Guggenheim Approach			Eötvös Approach		
	current study	Rebelo et al. ¹⁷	Weiss ³⁹	current study	Rebelo et al. ¹⁷	Weiss ³⁹
[C ₂ mim]Tf ₂ N	1300.3	1100	1300		1209	1570
[C ₄ mim]Tf ₂ N	1093.2	1012	1092		1077	1203
[C ₆ mim]Tf ₂ N	1156.1	932	1156		967	1303
[C ₈ mim]Tf ₂ N	1051.1					
[C ₈ mim]Tf ₂ N	917.7		920			950
[C ₁₀ mim]Tf ₂ N	875.8	800			797	
[C ₄ mim]Cl	1172.2			1159.6		
[C ₆ mim]Cl	1163.2			1214.4		
[C ₈ mim]Cl	1000.8	969		1020.1	931	
[C ₄ mim]PF ₆	1092.4	1102		1151.2	1187	
[C ₆ mim]PF ₆	1043.9	1050		1078.4	1109	
[C ₈ mim]PF ₆	988.4	972			997	
[C ₄ mim]BF ₄	1230.2	1158		1366.9	1240	
[C ₆ mim]BF ₄	1227.0			1339.2		
[C ₈ mim]BF ₄	1055.0	990		1189.7	1027	

also found a similar shift toward higher *T_c* values for [C_{*n*}mim]Tf₂N ILs (for *n* = 2, 4, 6, 8). The predicted *T_c* values obtained using both the Guggenheim and Eötvös approaches from this study, as well as the data from Rebelo et al.¹⁷ and Weiss,³⁹ are compared in Table 4. As the data demonstrate, in most cases, the Eötvös approach predicts a higher *T_c* value than the Guggenheim approach does.

Assuming that the plot of surface tension versus temperature is linear over the entire liquid range, the temperature at which $\gamma = 0$ was obtained using the available measured surface tensions at low temperature. This results in a hypothetical *T_c* value if the fluid at high temperatures, in the critical region, follows the linear behavior as well as it is followed at low temperatures. At low temperatures (e.g., $T \ll T_c$), the surface tension is given by the linear equation

$$\gamma = E^s - TS^s$$

where E^s is the surface excess energy and S^s is the surface excess entropy. It is well known that, for most fluids, both E^s and S^s are constants at $T \ll T_c$ and asymptotically vanish as T approaches T_c . If the linearity of surface tension at low

**Figure 1.** Plot of *T_c* values predicted by the Guggenheim approach versus E^s/S^s for the ionic liquids (ILs) in Table 1.

temperature is assumed to persist up to T_c , then $T'_c = E^s/S^s$ as $\gamma \rightarrow 0$, where the superscript prime indicates the hypothetical critical temperature obtained by the above assumption. Now, it can be proposed that a relationship exists between T_c and T'_c , the parameters of which are dependent on the theory used to predict T_c . The plot of T_c , predicted by the Guggenheim approach, versus T'_c for the ILs in Table 2 is shown in Figure 1. As it can be seen, T_c is related to T'_c linearly, e.g., $T_c = \alpha + \beta(E^s/S^s)$. Interestingly, the value of the slope β (1.223) is quite close to the value of the exponent in the Guggenheim relationship (e.g., 11/9). Only [C₈mim]PF₆ shows some deviation, which can be attributed to (i) the small number of data points that are available in the literature and (ii) the difference in the level of accuracy of the measurement. Note that the correlation between T_c and T'_c can be expected, since the behavior of a fluid near and far from of its critical temperature changes. The critical exponent, such as $\mu = 1.26$ for the surface tension (of most normal liquids), arises from the fact that the microscopic fluctuation around a mean property value in the T_c region becomes larger than the region far from T_c .

Table 5. Interaction Energies for the Studied ILs

	Interaction Energy, E_{inter} (kJ/mol)			
	BF_4^-	Cl^-	PF_6^-	I^-
$[\text{C}_4\text{mim}]^+$	-385.717	-380.280	-349.349	-340.724
$[\text{C}_6\text{mim}]^+$	-385.841	-375.639	-348.469	-341.253
$[\text{C}_8\text{mim}]^+$	-385.403	-374.943	-347.920	-340.272

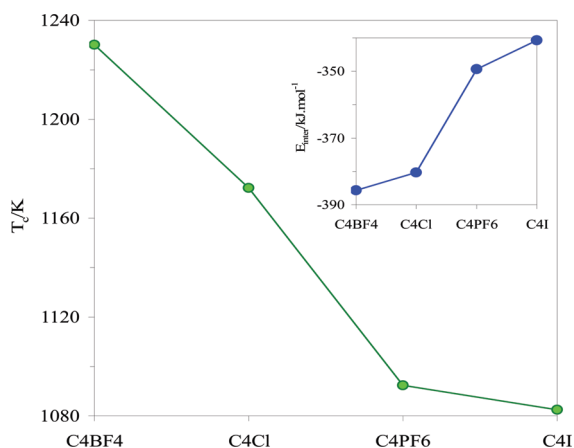
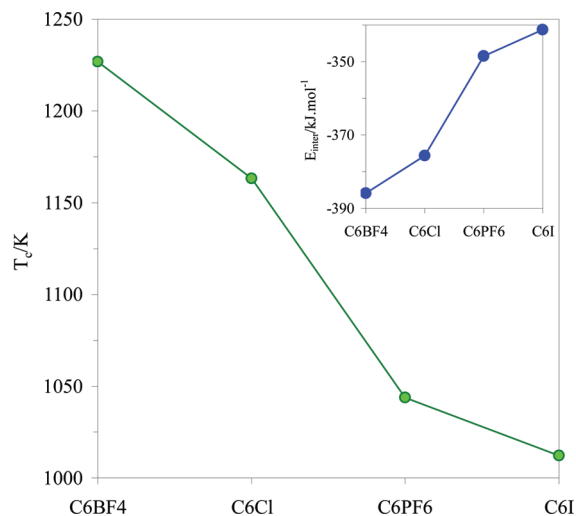
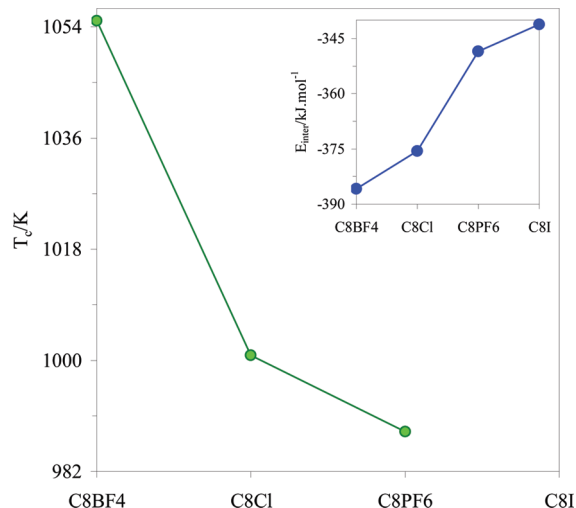
4.2. Correlation of the Critical Temperature (T_c) with the Interaction Energy. The T_c value is basically a measure of the intermolecular interaction potential energy (E_{inter}). The molecular internal degrees of freedom also contribute to these interactions. In the case of ILs, the major contribution comes from the anion–cation electrostatic interaction. In this section, we present the results of quantum mechanical calculations on the anion–cation interaction energies and study the correlation with the predicted critical-point temperatures. The calculated interaction energies are shown in Table 5. It can be seen that the influence of the anion type on the interaction energy is greater than that of the alkyl chain length. At the same time, the influence of the chain length on the interaction energy depends on the anion type. It is interesting to note that, by the present calculation, the interaction energies of ILs that have the BF_4^- anion remain almost unchanged as the chain length increases. The greatest effect of the chain length is observed in the case of chlorides. These ILs have not been analyzed previously for their interaction energies for the purpose of developing a correlation with the critical-point temperature.

The trend of the critical-point temperatures of different ILs is compared with their interaction energies in Figures 2–4. These figures show that the greater the interaction energy, the higher the critical-point temperature.

Table 3 shows that the T_c value for $[\text{C}_2\text{OHmim}]\text{BF}_4$ is the highest and, thus, a high interaction energy between its cation and the anion for this IL can be expected. Also, in phosphonium salts ($[\text{P}_{14}666]\text{Tf}_2\text{N}$ and $[\text{P}_{14}666]\text{Cl}$), as demonstrated in Table 3, the T_c values are the lowest values reported in this series of ILs, which suggests that the interaction energies between the cation and the anion for these ILs are weaker than the others.

5. Conclusions

The critical temperature of ionic liquids (ILs) has been predicted using the experimental surface tension data, based on the Eötvös method and the Guggenheim expression. Surface tension data measured both at liquid–vapor equilibrium and at ambient pressure were used. The critical temperature is a

**Figure 2.** Trend of predicted critical-point temperature, as a function of anion type, in 1-butyl-3-methyl imidazolium ILs. Inset shows the comparison with the trend of calculated E_{inter} values.**Figure 3.** Trend of predicted critical-point temperature, as a function of anion type, in 1-hexyl-3-methyl imidazolium ILs. Inset shows the comparison with the trend of calculated E_{inter} values.**Figure 4.** Trend of predicted critical-point temperature, as a function of anion type, in 1-octyl-3-methyl imidazolium ILs. Inset shows the comparison with the trend of calculated E_{inter} values.

function of the cation and anion types, as well as the alkyl chain length of the cation. The surface entropy is an important factor in the determination of the critical temperature, because it represents the temperature dependence of the surface tension. ILs with BF_4^- anion content, which have small surface entropies, 19a show high critical-point temperatures. The critical temperature decreases with the alkyl chain length. The cation–anion interaction energies, which were calculated by quantum mechanical computations, are correlated with the predicted critical temperature; ILs that have stronger cation–anion interactions have higher critical temperatures.

Plentiful data regarding the surface tension of many different ILs are available in the literature. Provided that the surface tension measurements that have been involved had good accuracies, the method shown in the present work shall provide a means of studying and confirming the trend of their interaction energies and their assessment, using the interaction energies.

Acknowledgment

The authors are indebted to the research council of Shiraz University for the financial support.

Literature Cited

- (1) Seddon, K. R. Room-Temperature Ionic Liquids: Neoteric Solvents for Clean Catalysis. *Kinet. Catal.* **1996**, *37*, 693–697.
- (2) Seddon, K. R. Ionic Liquids for Clean Technology. *J. Chem. Technol. Biotechnol.* **1997**, *68*, 351–356.
- (3) Freemantle, M. Designer Solvents. *Chem. Eng. News* **1998**, *76*, 32–37.
- (4) Rogers, R. D.; Seddon, K. R. Ionic Liquids-Solvents of the Future. *Science* **2003**, *302*, 792–793.
- (5) Dyson, P. J.; Ellis, D. J.; Welton, T.; Parker, D. G. Arene Hydrogenation in a Room-Temperature Ionic Liquid Using a Ruthenium Cluster Catalyst. *Chem. Commun.* **1999**, 25–26.
- (6) Martins, M. A. P.; Frizzo, C. P.; Moreira, D. N.; Zanatta, N.; Bonaccorso, H. G. Ionic Liquids in Heterocyclic Synthesis. *Chem. Rev.* **2008**, *108*, 2015–2050.
- (7) Hapiot, P.; Lagrost, C. Electrochemical Reactivity in Room-Temperature Ionic Liquids. *Chem. Rev.* **2008**, *108*, 2238–2264.
- (8) Dietz, M. L. Ionic Liquids as Extraction Solvents: Where Do We Stand? *Sep. Sci. Technol.* **2006**, *41*, 2047–2063.
- (9) Parvulescu, V. I.; Hardacre, Ch. Catalysis in Ionic Liquids. *Chem. Rev.* **2007**, *107*, 2615–2665.
- (10) Van Rantwijk, F.; Sheldon, R. A. Biocatalysis in Ionic Liquids. *Chem. Rev.* **2007**, *107*, 2757–2785.
- (11) Wasserscheid, P.; Welton, T. Eds. *Ionic Liquids in Synthesis*; Wiley–VCH: Weinheim, Germany, 2002.
- (12) Zhang, S.; Sun, N.; He, X.; Lu, X.; Zhang, X. Physical Properties of Ionic Liquids: Database and Evaluation. *J. Phys. Chem. Ref. Data* **2006**, *35*, 1475–1517.
- (13) Domanska, U.; Krolkowska, M. Effect of Temperature and Composition on the Surface Tension and Thermodynamic Properties of Binary Mixtures of 1-Butyl-3-Methylimidazolium Thiocyanate with Alcohols. *J. Colloid Interface Sci.* **2010**, *348*, 661–667.
- (14) (a) Valderrama, J. O.; Robles, P. A. Critical Properties, Normal Boiling Temperatures, and Acentric Factors of Fifty Ionic Liquids. *Ind. Eng. Chem. Res.* **2007**, *46*, 1338–1344. (b) Valderrama, J. O.; Sanga, W. W.; Lazzús, J. A. Critical Properties, Normal Boiling Temperature, and Acentric Factor of Another 200 Ionic Liquids. *Ind. Eng. Chem. Res.* **2008**, *47*, 1318–1330.
- (15) Widom, B. Surface Tension and Molecular Correlations near the Critical point. *J. Chem. Phys.* **1965**, *43*, 3892–3897.
- (16) Fisk, S.; Widom, B. Structure and Free Energy of the Interface between Fluid Phases in Equilibrium near the Critical Point. *J. Chem. Phys.* **1969**, *50*, 3219–3227.
- (17) Rebelo, L. P. N.; Lopes, J. N. C.; Esperanca, J. M. S. S.; Filipe, E. On the Critical Temperature, Normal Boiling Point, and Vapor Pressure of Ionic Liquids. *J. Phys. Chem. B* **2005**, *109*, 6040–6043.
- (18) Weiss, V. C.; Heggen, B.; Muller-Plathe, F. Critical Parameters and Surface Tension of the Room Temperature Ionic Liquid [bmim][PF₆]: A Corresponding-States Analysis of Experimental and New Simulation Data. *J. Phys. Chem. C* **2010**, *114*, 3599–3608.
- (19) (a) Ghatee, M. H.; Zolghadr, A. R. Surface Tension Measurements of Imidazolium-Based Ionic Liquids at Liquid–Vapor Equilibrium. *Fluid Phase Equilib.* **2008**, *263*, 168–175. (b) Ghatee, M. H.; Zare, M.; Moosavi, F.; Zolghadr, A. R. Temperature-Dependent Density and Viscosity of the Ionic Liquids 1-Alkyl-3-methylimidazolium Iodides: Experiment and Molecular Dynamics Simulation. *J. Chem. Eng. Data* **2010**, *55*, 3084–3088.
- (20) Carvalho, P. J.; Neves, C. M. S. S.; Coutinho, J. A. P. Surface Tensions of Bis(trifluoromethylsulfonyl)imide Anion-Based Ionic Liquids. *J. Chem. Eng. Data* **2010**, *55*, 3807–3812.
- (21) Turner, E. A.; Pye, C. C.; Singer, R. D. Use of ab Initio Calculations toward the Rational Design of Room Temperature Ionic Liquids. *J. Phys. Chem. A* **2003**, *107*, 2277–2288.
- (22) Ghatee, M. H.; Maleki, A.; Ghaed-Sharaf, H. Extended Generic Nature of Surface Entropy. *Langmuir* **2003**, *19*, 211–213.
- (23) Wu, X. Z.; Ocko, B. M.; Sirota, E. B.; Sinha, S. K.; Deutsch, M.; Cao, B. H.; Kim, M. W. Surface Tension Measurements of Surface Freezing in Liquid Normal Alkanes. *Science* **1993**, *261*, 1018–1021.
- (24) (a) Ghatee, M. H.; Soorghali, A. Application of Extended Scaling Law to the Surface Tension of Fluids of Wide Range of Molecular Shapes. *Fluid Phase Equilib.* **2006**, *249*, 153–158. (b) Miqueua, C.; Broseta, D.; Satherley, J.; Mendiboure, B.; Lachaise, J.; Graciaa, A. An extended scaled equation for the temperature dependence of the surface tension of pure compounds inferred from an analysis of experimental data. *Fluid Phase Equilib.* **2000**, *172*, 169–182.
- (25) Guggenheim, E. A. The Principle of Corresponding States. *J. Chem. Phys.* **1945**, *13*, 253–261.
- (26) Frisch, M. J.; Trucks, G. W.; Schlegel, H. B.; Scuseria, G. E.; Robb, M. A.; Cheeseman, J. R.; Montgomery, J. A., Jr.; Vreven, T.; Kudin, K. N.; Burant, J. C.; Millam, J. M.; Iyengar, S. S.; Tomasi, J.; Barone, V.; Mennucci, B.; Cossi, M.; Scalmani, G.; Rega, N.; Petersson, G. A.; Nakatsuji, H.; Hada, M.; Ehara, M.; Toyota, K.; Fukuda, R.; Hasegawa, J.; Ishida, M.; Nakajima, T.; Honda, Y.; Kitao, O.; Nakai, H.; Klene, M.; Li, X.; Knox, J. E.; Hratchian, H. P.; Cross, J. B.; Bakken, V.; Adamo, C.; Jaramillo, J.; Gomperts, R.; Stratmann, R. E.; Yazyev, O.; Austin, A. J.; Cammi, R.; Pomelli, C.; Ochterski, J. W.; Ayala, P. Y.; Morokuma, K.; Voth, G. A.; Salvador, P.; Dannenberg, J. J.; Zakrzewski, V. G.; Dapprich, S.; Daniels, A. D.; Strain, M. C.; Farkas, O.; Malick, D. K.; Rabuck, A. D.; Raghavachari, K.; Foresman, J. B.; Ortiz, J. V.; Cui, Q.; Baboul, A. G.; Clifford, S.; Cioslowski, J.; Stefanov, B. B.; Liu, G.; Liashenko, A.; Piskorz, P.; Komaromi, I.; Martin, R. L.; Fox, D. J.; Keith, T.; Al-Laham, M. A.; Peng, C. Y.; Nanayakkara, A.; Challacombe, M.; Gill, P. M. W.; Johnson, B.; Chen, W.; Wong, M. W.; Gonzalez, C.; Pople, J. A. *Gaussian 03, revision C.02*; Gaussian, Inc.: Wallingford, CT, 2004.
- (27) (a) Del Popolo, M. G.; Lynden-Bell, R. M.; Kohanoff, J. Ab Initio Molecular Dynamics Simulation of a Room Temperature Ionic Liquid. *J. Phys. Chem. B* **2005**, *109*, 5895–5902. (b) Kossmann, S.; Thar, J.; Kirchner, B.; Hunt, P. A.; Welton, T. Cooperativity in Ionic Liquids. *J. Chem. Phys.* **2006**, *124*, 174506.
- (28) Pereiro, A. B.; Legido, J. L.; Rodriguez, A. Physical Properties of Ionic Liquids Based on 1-Alkyl-3-Methylimidazolium Cation and Hexafluorophosphate as Anion and Temperature Dependence. *J. Chem. Thermodyn.* **2007**, *39*, 1168–1175.
- (29) Klomfar, J.; Souckova, M.; Patek, J. Surface Tension Measurements for Four 1-Alkyl-3-methylimidazolium-Based Ionic Liquids with Hexafluorophosphate Anion. *J. Chem. Eng. Data* **2009**, *54*, 1389–1394.
- (30) Restolho, J.; Serro, A. P.; Mata, J. L.; Saramago, B. Viscosity and Surface Tension of 1-Ethanol-3-methylimidazolium Tetrafluoroborate and 1-Methyl-3-octylimidazolium Tetrafluoroborate over a Wide Temperature Range. *J. Chem. Eng. Data* **2009**, *54*, 950–955.
- (31) Kilaru, P.; Baker, G. A.; Scovazzo, P. Density and Surface Tension Measurements of Imidazolium-, Quaternary Phosphonium-, and Ammonium-Based Room-Temperature Ionic Liquids: Data and Correlations. *J. Chem. Eng. Data* **2007**, *52*, 2306–2314.
- (32) Tong, J.; Liu, Q.; Zhang, P.; Yang, J. Surface Tension and Density of 1-Methyl-3-hexylimidazolium Chloroindium. *J. Chem. Eng. Data* **2007**, *52*, 1497–1500.
- (33) Carvalho, P. J.; Freire, M. G.; Marrucho, I. M.; Queimada, A. J.; Coutinho, J. A. P. Surface Tensions for the 1-Alkyl-3-methylimidazolium Bis(trifluoromethylsulfonyl)imide Ionic Liquids. *J. Chem. Eng. Data* **2008**, *53*, 1346–1350.
- (34) Wandschneider, A.; Lehmann, J. K.; Heintz, A. Surface Tension and Density of Pure Ionic Liquids and Some Binary Mixtures with 1-Propanol and 1-Butanol. *J. Chem. Eng. Data* **2008**, *53*, 596–599.
- (35) Pereiro, A. B.; Santamarta, F.; Tojo, E.; Rodriguez, A.; Tojo, J. Temperature Dependence of Physical Properties of Ionic Liquid 1,3-Dimethylimidazolium Methyl Sulfate. *J. Chem. Eng. Data* **2006**, *51*, 952–954.
- (36) Pereiro, A. B.; Verdia, P.; Tojo, E.; Rodriguez, A. Physical Properties of 1-Butyl-3-methylimidazolium Methyl Sulfate as a Function of Temperature. *J. Chem. Eng. Data* **2007**, *52*, 377–380.
- (37) Gomez, E.; Gonzalez, B.; Calvar, N.; Tojo, E.; Dominguez, A. Physical Properties of Pure 1-Ethyl-3-methylimidazolium Ethylsulfate and Its Binary Mixtures with Ethanol and Water at Several Temperatures. *J. Chem. Eng. Data* **2006**, *51*, 2096–2102.
- (38) Liu, Q.; Tong, J.; Tan, Z.; Welz-Biermann, U.; Yang, J. Density and Surface Tension of Ionic Liquid [C_mmim][PF₆(CF₃CF₃)₃] and Prediction of Properties [C_mmim][PF₆(CF₃CF₃)₃] (*n* = 1, 3, 4, 5, 6). *J. Chem. Eng. Data* **2010**, *55*, 2586–2589.
- (39) Weiss, V. C. Guggenheim's Rule and the Enthalpy of Vaporization of Simple and Polar Fluids, Molten Salts, and Room Temperature Ionic Liquids. *J. Phys. Chem. B* **2010**, *114*, 9183–9194.

Received for review June 28, 2010

Revised manuscript received October 8, 2010

Accepted October 11, 2010

IE1013772